EUROPHYSICS LETTERS 1 August 2002

Europhys. Lett., **59** (3), pp. 410–416 (2002)

Anchoring and orientational wetting of nematic liquid crystals on semi-fluorinated self-assembled monolayer surfaces

B. Alkhairalla[1], N. Boden[1], E. Cheadle[1], S. D. Evans[1](*), J. R. Henderson[1], H. Fukushima[2], S. Miyashita[2], H. Schönherr[3], G. J. Vancso[3], R. Colorado jr[4], M. Graupe[4], O. E. Shmakova[4] and T. R. Lee[4]

[1] *Centre for Self-Organising Molecular Systems, University of Leeds Leeds, LS2 9JT, UK*
[2] *Base Technology Research Centre, Seiko-Epson Co - Nagano-ken, Japan*
[3] *University of Twente, MESA$^+$ Research Institute and Faculty of Chemical Technology, MTP - P.O. Box 217, 7500 AE Enschede, The Netherlands*
[4] *Department of Chemistry, University of Houston Houston, TX, 77204-5641, USA*

(received 19 November 2001; accepted in final form 14 May 2002)

PACS. 64.70.Md – Transitions in liquid crystals.
PACS. 68.35.Rh – Phase transitions and critical phenomena.
PACS. 68.08.-p – Liquid-solid interfaces.

Abstract. – We demonstrate that it is possible to achieve exceptionally fine control over the anchoring of liquid crystals via the use of semi-fluorinated self-assembled monolayers of varying spacer length. We use this approach to map the detailed shape of an anchoring transition surface in thermodynamic phase space and to explore the links between anchoring and orientational wetting phenomena. These results allow one to design a substrate that will place a standard liquid-crystal film arbitrarily close to an anchoring transition between homeotropic and planar anchoring.

The anchoring of liquid crystals [1, 2], whereby the nematic director is pinned to be perpendicular (homeotropic) or parallel (planar) to a substrate, is extremely important technologically, from the display perspective, for the development of novel chemical and biological sensors, and for the use of liquid crystals as templates for the production of inorganic materials [3, 4]. The nature of the anchoring observed is highly sensitive to the delicate balance of forces arising from surface roughness, chemical composition, surface anisotropy, surface elasticity, surface charge, etc. In this letter we address this issue by generating model experimental systems for the systematic study of the physics of anchoring. Of greatest importance, both technically and fundamentally, is to understand how to control the orientational order of adsorbed liquid crystalline films. This information can then be expressed in terms of a phase diagram [5,6]. In our work the axes of this phase space are temperature (T), molecular length of the alkyl chain of the liquid-crystal molecules (n) and the substrate field (h_1). The latter quantity is any convenient measure of the surface energy of the substrate (*e.g.*, hydrophobic *vs.* hydrophilic expressed in terms of a contact angle for adsorbed water drops). As far as we

(*) E-mail: s.d.evans@leeds.ac.uk

Table I – *Structure and properties of the SAM substrates used in this study.*

Short name	Compound	Water contact angles ($\pm 2^\circ$)		Lattice spacing
		θ_{adv}	θ_{rec}	(Å)
A1	$[S(CH_2)_2OCO(CF_2)_8CF_3]_2$	117	107	5.7 ± 0.2
A2	$[S(CH_2)_6OCO(CF_2)_8CF_3]_2$	120	108	5.7 ± 0.1
A3	$[S(CH_2)_{11}OCO(CF_2)_8CF_3]_2$	119	109	5.7 ± 0.1
B1	$HS(CH_2)_2(CF_2)_9CF_3$	119	109	5.8
B2	$HS(CH_2)_6(CF_2)_9CF_3$	117	108	5.8
B3	$HS(CH_2)_{11}(CF_2)_9CF_3$	119	111	5.9
B4	$HS(CH_2)_{17}(CF_2)_9CF_3$	118	110	$6.1, 6.6, 7.1$
B5	$HS(CH_2)_{33}(CF_2)_9CF_3$	119	108	$8.2, 7.1, 8.3$

know, the fine details of this phase behavior, the physics of anchoring, are unexplored experimentally. A far better understood class of phase transitions are the wetting transitions, from partial to complete, and the approach to complete or partial wetting from off-bulk two-phase coexistence. The latter is directly analogous to an adsorption isotherm, only here the system is approaching bulk isotropic nematic coexistence ($T \to T_{\mathrm{IN}}$ from above) and one notes whether or not a film of nematic grows at the substrate isotropic interface. If the thickness of such a film grows arbitrarily large as T reduces to T_{IN} then at T_{IN} the nematic phase is said to completely wet the substrate isotropic interface. Detailed theoretical predictions are available for this behaviour [7]. Otherwise, this interface is only partially wet or non-wet by nematic. In the global phase diagram, the wetting transition occurs at T_{IN}, for n and h_1 such that partial wetting and complete wetting coexist (first-order wetting) or merge (critical wetting). Since the associated order parameter is dominated by the orientational order of the adsorbed film, rather than the density difference with the isotropic phase, this class of wetting transition is often referred to as orientational wetting phenomena. In contrast to orientational wetting transitions ($T = T_{\mathrm{IN}}$) and the approach to orientational wetting ($T > T_{\mathrm{IN}}$), an anchoring transition occurs at the substrate/nematic interface ($T < T_{\mathrm{IN}}$). When expressed as a phase diagram, this means that the anchoring transition surface ends at isotropic nematic coexistence (T_{IN}), potentially as a line of orientational wetting transitions. It is therefore of considerable interest to ask if/when anchoring is directly linked to orientational wetting [5, 6]. It is also worth noting that the future will see increasing research into the use of patterned substrates to induce additional control over interfacial phenomena. For example, patterns of homeotropic contrasting with planar anchoring can be readily observed on the micrometer scale [8].

To focus on the nature of the anchoring transition close to bulk isotropic/nematic (I/N) coexistence we chose two specific series of self-assembled monolayer (SAM) substrates formed from semi-fluorinated thiol and disulphide derivatives, respectively. The structural properties of SAMs formed from such compounds have been thoroughly investigated by experiments that show that close-packed monolayers are formed with the perfluorocarbon chains nearly normal to the surface ($< 16^\circ$) and arranged on a hexagonal lattice with a nearest-neighbor spacing of about 5.8 Å [9–13]. Thus, in terms of the terminal functionality (and nearby underlying groups) all of our surfaces are identical. Essentially, the SAM molecules used in this study differ only in the length of the lower hydrocarbon portion. Thus, the parameter being controlled, assuming all other factors remain constant, is the separation of the LC/SAM interface from the underlying gold surface to which the SAM molecules are bonded. In principle, the only consequence of this control is a varying contribution from the dispersion forces associated with the underlying metallic substrate [14–16]. Since the SAM chain lengths are relatively large this variation will be exceptionally weak, in effect acting as a fine-control tuner for the

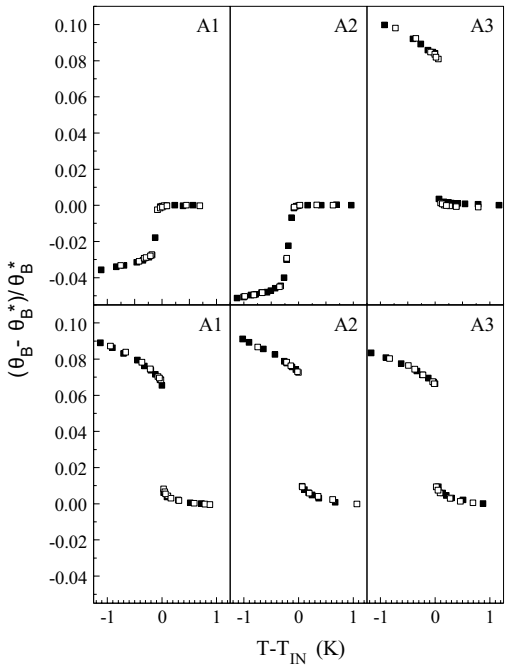

Fig. 1

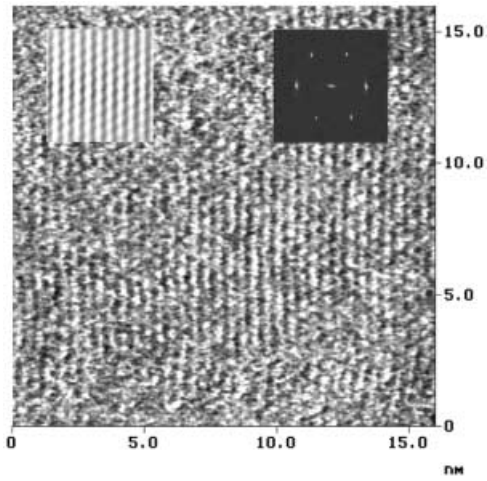

Fig. 2

Fig. 1 – Brewster angle data (θ_B), normalized to the value at $T \gg T_{IN}$ (θ_B^*), for orientational wetting and anchoring of 5CB (top set) and 6CB (bottom set) on SAMs formed from compounds A1, A2, and A3. Both heating (open squares) and cooling (solid squares) runs are shown.

Fig. 2 – An AFM image of the fluorinated disulphide SAM labeled A1 in table I. The insets show an image-enhanced structure and the reciprocal lattice, respectively.

h_1 field. The two series of SAMs investigated are listed in table I, together with standard measurements of advancing and receding water contact angles, and the lattice spacing obtained from AFM measurements carried out for this study. An evanescent-wave ellipsometric technique was used to follow the anchoring and orientational wetting behavior of the LCs. Here the average orientational order within the evanescent field can be obtained by simply measuring the Brewster angle, θ_B, which in this surface-sensitive technique lies above the critical angle. For full details of our experimental set-up we refer the reader to previous publications [5, 6]. Briefly, the appearance of a nematic film at the substrate/isotropic interface leads to a shift in the Brewster angle. This arises because the presence of an oriented film of polar molecules will strongly influence the dielectric properties of a medium probed by polarised light. In the evanescent mode, this shift is linear in the thickness of the adsorbed film, for thicknesses significantly less than the wavelength of the light and the decay length of the evanescent field, and is readily modelled by standard optical techniques based on Fresnel's relations [5,6]. Of special importance to our study is the fact that this shift is of opposite sign between homeotropic *vs.* planar orientation. Thus, simply monitoring the Brewster angle as a function of $T \to T_{IN}$ from above tells us whether or not a nematic film is growing at the substrate isotropic interface and, if so, what the orientation of the nematic director is. At $T < T_{IN}$ the value of θ_B is similarly determined by the orientation of the molecules within the evanescent field. Thus, our technique is also a surface-sensitive tool for identifying the anchoring direction at a substrate nematic interface and for detecting anchoring transitions. The raw data presented in figs. 1 and 3 below therefore display all the information needed to

construct the anchoring and orientational wetting phase diagram, without any modelling or further processing required.

The isotropic/nematic phase transition, $T_{\rm IN}$, was approached by slowly cooling from the isotropic phase into the nematic phase and, subsequently, heating to the isotropic phase to check for hysteresis. At this stage a temperature range of only $\pm 1^\circ$ about $T_{\rm IN}$ was explored. The alkylcyanobiphenyl LC molecules 5CB and 6CB were used, since we knew from our earlier studies that these systems would lie very close to, if not on opposite sides of, an anchoring transition surface. Figure 1 presents these data for a range of surfaces. From the introductory discussion above we can immediately read off the anchoring direction at $T < T_{\rm IN}$ and detect the growth of oriented films at $T > T_{\rm IN}$. For example, in fig. 1, 5CB on A1, $\theta_{\rm B}$ is constant at $T > T_{\rm IN}$, appropriate to partial wetting or non-wetting (no observable film growth). In contrast, fig. 1, 6CB on A1, shows $\theta_{\rm B}$ increasing smoothly as $T \to T_{\rm IN}$ from above, consistent with an approach to complete wetting (the continuous growth of a homeotropic film). For a detailed analysis of the divergent nature of this film growth the reader is referred to ref. [6]. Variations in $\theta_{\rm B}$ at $T < T_{\rm IN}$ are reflecting changes in the anchoring strength as the transition to isotropic bulk phase is approached.

Thus, from fig. 1 in the case of 5CB on SAMs A1 and A2, we find planar alignment at $T < T_{\rm IN}$, with perhaps some difference in the anchoring strengths. At $T > T_{\rm IN}$, these data are in accord with non-wetting or partial wetting by nematic at the isotropic/SAM interface ($\theta_{\rm B}$ is constant). For 5CB on SAM A3, however, fig. 1 shows homeotropic anchoring, which grows stronger as the temperature is reduced. In the case of 6CB, we find homeotropic anchoring at $T_{\rm IN}$ on all three surfaces. Here, we observe a continuous increase in $\theta_{\rm B}$ and hence the continuous growth of a nematic film as the temperature is reduced toward $T_{\rm IN}$; *i.e.*, an approach to complete orientational wetting at the isotropic/SAM interface. The system 5CB on A3 must lie very close to the wetting transition marking the boundary of complete wetting. We tentatively ascribe the marked reduction in the magnitude of the nematic film growth at $T > T_{\rm IN}$ to a significantly weaker 5CB-5CB pairing interaction, leading to a reduction in the driving force for homeotropic anchoring.

Our previous investigations of the T, n, h_1, phase diagram [5, 6] show that homeotropic anchoring of nCB molecules is associated with low-energy surfaces [17] whereas high-energy surfaces promote planar anchoring [5,6]. Thus, our latest results suggest that the SAM formed from A3 presents a lower-energy surface than those of A1 and A2, which is at least consistent with the significantly longer hydrocarbon spacer-link (the LC lies further from the gold). However, macroscopic contact angle data (table I) cannot distinguish between these surfaces. In light of these considerations, we have attempted to rule out differences on the molecular level, between the outer surfaces of these three SAMs. The CF_3 tail group lattice structures of the SAMs (all bonded to Au(111)) were imaged using atomic-force microscopy (AFM). The edges of the triangular Au(111) terraces correspond to next-neighbour directions of the Au(111) lattice. By comparing the direction of the edges and the direction of the observed lattices, the relative orientation of the tail group lattice with respect to the underlying Au(111) could be determined [18]. All three SAMs displayed hexagonal lattice structures with a lattice constant of 5.7 Å (fig. 2). However, the relative orientation of the tail group lattice with respect to the underlying Au(111) was found to depend on the length of the alkane spacer-segment between the disulphide and the ester groups. While the short-chain compounds with 2 and 6 methylene units form a $p(2 \times 2)$ tail group lattice (fig. 2), the compound with $n = 11$ forms a $c(7 \times 7)$ structure as has been observed previously for fluorinated thiols and disulphides [13,18].

The above findings raise the question as to whether the observed differences in anchoring are governed by the increase in separation from the underlying gold support or if instead they are due to variation of the short-ranged interaction caused by the relative orientation of the

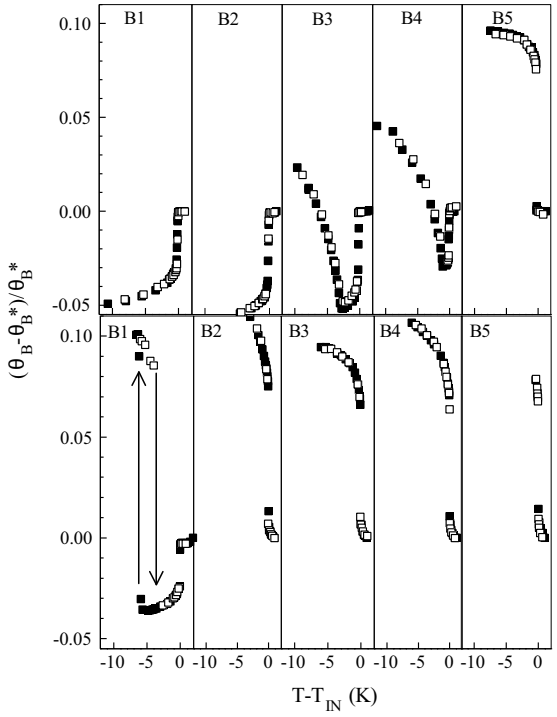

Fig. 3

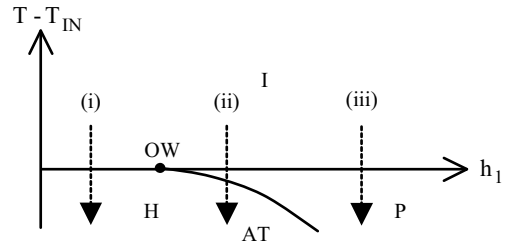

Fig. 4

Fig. 3 – Brewster angle data (θ_B), normalized to the value at $T \gg T_{IN}$ (θ_B^*), for orientational wetting and anchoring of 5CB (top set) and 6CB (bottom set) on SAMs formed from compounds B1 to B5 (table I). Both heating (open squares) and cooling (solid squares) runs are shown. The vertical lines joining the data for 6CB on B1 indicate hysteresis.

Fig. 4 – Schematic representation of our data, in the form of a fixed-n slice through (T, n, h_1) phase space (see text).

SAM lattice with respect to that of the gold. The results presented below favor the former explanation. In any case our work demonstrates that the anchoring is sensitive to subtle changes in the surface free energy that cannot be detected with macroscopic contact angle measurements.

To probe the anchoring transition surface below T_{IN}, the series of SAM materials B1-B5 in table I were used. These systems had an upper perfluorocarbon chain of fixed length and a lower hydrocarbon portion of variable length and were studied over a wider temperature range. The data are collected in fig. 3. Considering the 5CB experiments first, it is evident that on SAMs B1 and B2 planar anchoring is found and that the Brewster angle decreases slowly as T decreases well below T_{IN} (again probably associated with variation of the anchoring strength). On substrate B5, formed with the longest alkyl chain, only homeotropic alignment was found. For the surfaces formed with compounds of intermediate length the anchoring transition for 5CB lies within our experimental range. Initially, as T was cooled below T_{IN}, planar anchoring was observed. However, on continued cooling the samples underwent an anchoring transition from planar to homeotropic. These processes were reversible, with perhaps evidence of weak hysteresis at the change in anchoring just observable. The difference in temperature, $T_A - T_{IN}$, between the anchoring transition T_A and the bulk isotropic/nematic transition, decreases with increasing hydrocarbon spacer length until the anchoring transition terminates at T_{IN}. On

SAMs of even larger thickness, the LC goes straight from isotropic to the homeotropic-nematic phase. That is, for B1-B5 the anchoring transition is moving to higher temperature as the SAM thickness increases.

The 6CB data show that for this LC the orientational wetting transition lies between B1 and B2; *i.e.* all the systems B2 to B5 involve a continuous growth of nematic film as T tends to $T_{\rm IN}$ from above. The system 6CB on B1 shows no growth of nematic at $T > T_{\rm IN}$ and displays a region of planar anchoring before undergoing a clear first-order anchoring transition (note the hysteresis). The data of fig. 3 imply that increasing the alkyl chain length of the SAM (reducing the long-range dispersion interaction with the gold) enhances the tendency toward homeotropic anchoring. The shape of the anchoring transition surface in (T, n, h_1) space is such that, for a given system (fixed n and h_1), one crosses from planar to homeotropic by lowering the temperature. To confirm this scenario, we returned to one of the previous samples (5CB on A2) and found similar behaviour by extending the temperature range of the data.

AFM studies of the SAMs formed from compounds B1-B5 yielded lattice constants that increased with increasing alkyl-chain spacer length and produced a change in the observed lattice from hexagonal (B1-B3) to distorted hexagonal (B4, B5); see table I. While this might be associated with an increase in the tilt of the perfluorocarbon chain, the ellipsometrically determined thicknesses of the SAMs showed a linear dependence with the number of CH_2 units, implying that any such changes must be small. The effect of increasing the molecular tilt would probably be to increase the surface free energy since the ratio of CF_2 to CF_3 groups presented at the surface would be increased. Accordingly, we would expect any such difference in surface free energy to cause the onset of the transition to homeotropic anchoring to be delayed. That the opposite actually happens suggests that the variation in the long-range interaction with the gold substrate is dominating the changes in anchoring.

Thus, we conclude that SAMs formed from perfluorocarbon derivatives produce highly ordered and chemically well-defined surfaces for studying the anchoring of calamitic liquid crystals. The liquid crystals 5CB and 6CB undergo an anchoring transition from planar to homeotropic at temperatures below the bulk isotropic/nematic transition. By increasing the separation of the LC/SAM interface from the underlying gold substrate, the anchoring transition is shifted from lower to higher temperatures until it terminates at the bulk isotropic/nematic transition temperature. The anchoring transition is clearly first-order for 6CB, but is significantly weaker for 5CB.

In a previous publication [6], we presented the simplest generic (T, n, h_1) phase diagram for describing the orientational alignment of nCB molecules on gold/thiol SAM substrates. In the study presented here, we have explored a greatly magnified region of this phase space, by looking at tiny variations of h_1. Figure 4 shows a schematic fixed-n cut through this phase diagram, in the light of our current experimental data. On the basis of the 6CB data, we have drawn a first-order anchoring transition line (AT) terminating at a continuous orientational wetting transition (OW) at $T = T_{\rm IN}$. For values of h_1 (here controlled by the spacer length of our SAMs) less than the value at OW, lowering T toward $T_{\rm IN}$ yields an approach to complete wetting by homeotropic-nematic at the substrate/isotropic interface (path (i)). For values of h_1 greater than the value at OW, there is no indication of wetting at $T > T_{\rm IN}$ and an experimental path down the temperature axis crosses abruptly at $T_{\rm IN}$ into a planar anchoring regime; see paths (ii) and (iii) in fig. 4. At even lower temperatures, if h_1 is not too far beyond the value at OW, the experiment will intersect the anchoring transition surface from planar to homeotropic; see path (ii). Note that the slope with which the AT line joins OW is not yet known from experiment so our choice in fig. 4 is based on a possible interpretation of the generalized Clapeyron equation defining the slope of the AT curve. Our data are currently consistent with a continuous orientational wetting transition; *i.e.* there is no sign of

a prewetting transition line at $T > T_{\mathrm{IN}}$ for $h_1 <$ OW. Given additional SAMs of intermediate spacer length it should be possible to confirm whether or not the first-order character of the AT surface disappears at OW.

The above scenario assumes that the substrate is an entirely benign spectator phase; *e.g.*, no T-dependence to the SAM structure and no interpenetration of the LC molecules into the SAMs. It is interesting that our phase diagram is in agreement with a long-standing empirical rule, based on careful early experiments, that "homeotropic anchoring occurs whenever the substrate surface energy is less than the liquid-vapor surface tension of the LC fluid (attributed to the domination of fluid-fluid interactions)" [19]. We believe this early work to be directly relevant to our systems, in contrast to a recent analysis of anchoring on Langmuir-Blodgett films for which the elastic response of the substrate plays a key role [20].

* * *

The work at the University of Houston was supported by the National Science Foundation (DMR-9700662) and by Seiko Epson Corporation. BA and EC would like to thank the EPSRC for the provision of PhD studentships. EC also acknowledges Seiko Epson for the provision of a CASE award.

REFERENCES

[1] de Gennes P. G., *The Physics of Liquid Crystals* (Clarendon Press, Oxford) 1974.
[2] Jerome B., *Rep. Prog. Phys.*, **54** (1991) 391.
[3] Gupta V. K., Skaife J. J., Dubrovsky T. B. and Abbott N. L., *Science*, **279** (1998) 2077.
[4] Attard G. S., Bartlett P. N., Coleman N. R. B., Elliott J. M., Owen J. R. and Wang J. H., *Science*, **278** (1997) 838.
[5] Evans S. D., Allinson H., Boden N. and Henderson J. R., *Faraday Discuss.*, **104** (1996) 37.
[6] Alkhairalla B., Allinson H., Boden N., Evans S. D. and Henderson J. R., *Phys. Rev. E*, **59** (1999) 3033.
[7] Sullivan D. E. and Lipowsky R., *Can. J. Chem.*, **66** (1988) 553.
[8] Cheng Y. L., Henderson J. R., Evans S. D. and Lydon J., *Liq. Cryst.*, **27** (2000) 1267.
[9] Fukushima H., Seki S., Nishikawa T., Takiguchi H., Tamada K., Abe K., Colorado R. jr, Graupe M., Shmakova O. E. and Lee T. R., *J. Phys. Chem. B*, **104** (2000) 7417.
[10] Schönherr H., Ringsdorf H., Jaschke M., Butt H.-J., Bamberg E., Allinson H. and Evans S. D., *Langmuir*, **12** (1996) 3898.
[11] Liu G.-Y., Fenter P., Chisdey C. E. D., Ogletree D. F., Eisenberger P. and Salmeron M., *J. Chem. Phys.*, **101** (1994) 4301.
[12] Alves C. A. and Porter D., *Langmuir*, **9** (1993) 3507.
[13] Jaschke M., Schönherr H., Wolf H., Butt H.-J., Bamberg E., Besocke M. K. and Ringsdorf H., *J. Phys. Chem.*, **100** (1996) 2290.
[14] Miller W. J. and Abbott N. L., *Langmuir*, **13** (1997) 7106.
[15] Landau L. D. and Lifshitz E. M., *Electrodynamics of Continuous Media* (Pergamon Press, New York) 1960.
[16] Israelachvili J., *Intermolecular and Surface Forces* (Academic Press, San Diego) 1976.
[17] By low-energy surfaces we are referring to those with surface free energies typically associated with perfluorinated materials, *i.e.*, $\leq 12\,\mathrm{mJ\,m^{-2}}$.
[18] Nelles G., Schönherr H., Jaschke M., Wolf H., Schaub M., Küther J., Tremel W., Bamberg E., Ringsdorf H. and Butt H.-J., *Langmuir*, **14** (1998) 808.
[19] Creagh L. T. and Kmetz A. R., *Mol. Crys. Liq. Cryst.*, **24** (1973) 59.
[20] Alexeionescu A. L., Barberi R., Barbero G., Bonvent J. J. and Giocondo M., *Appl. Phys. A*, **61** (1995) 425 and references therein.